Microcrystalline *n-i-p* tunnel junction in *a*-Si:H/*a*-Si:H tandem cells

F. A. Rubinelli
INTEC, Universidad Nacional del Litoral, Güemes 3450, 3000 Santa Fe, Argentina

J. K. Rath and R. E. I. Schropp
Utrecht University, Debye Institute, P.O. Box 80000, 3508 TA Utrecht, The Netherlands

(Received 19 June 2000; accepted for publication 4 January 2001)

The kinetics controlling the electrical transport inside the μc-Si tunnel-recombination junction (TRJ) of *a*-Si:H/*a*-Si:H tandem solar cells was studied in detail with computer simulations. Trap assisted recombination tunneling and Poole–Frenkel mechanisms were included in our analysis. Three different μc-Si tunnel junctions were investigated: (a) *n-p*, (b) *n*-oxide-*p* and (c) *n-i-p*. The highest theoretical efficiencies in *a*-Si:H/*a*-Si:H tandem cells were achieved with the *n-i-p* tunnel junction structure. The impact of the μc-Si effective masses, mobility gap, and mobilities in the tandem solar cell efficiency is also studied in this article. Several *a*-Si:H/*a*-Si:H tandem solar cells were made with the μc-Si tunnel configurations of types (b) and (c). In all of these samples one extra oxide layer was needed at the *i*-*a*-Si:H/*n*-μc-Si interface. Both tunnel junctions lead us to comparable experimental tandem solar cell efficiencies. When the *n-i-p* structure is implemented as TRJ in the *a*-Si:H/*a*-Si:H tandem solar cell, efficiencies sensitively depend upon the tunnel junction intrinsic layer thickness. The optimization of this thickness provides a more controlled way of maximizing the tandem solar cell efficiency. Illuminated $J-V$ and QE characteristics were successfully fitted using computer modeling. © *2001 American Institute of Physics.*
[DOI: 10.1063/1.1352032]

I. INTRODUCTION

Hydrogenated amorphous silicon (*a*-Si:H/*a*-Si:H) stacked tandem solar cells have received considerable attention in the last few years because they are more robust to light soaking than single *a*-Si:H *p-i-n* heterojunctions. Using controlled deposition conditions the *a*-Si:H mobility gap can be conveniently tailored at the top and bottom cells to use the sunlight spectrum more efficiently. Bruns *et al.*[1] studied the current matching of *a*-Si:H stacked cells by measuring the spectral response (QE) under different bias lights and voltages. In their simulations they add an interface region between the doped *n*-*a*-Si:H and *p*-*a*-Si:H layers where the mobility gap is only 0.62 eV in order to obtain realistic spectral responses. Wieder *et al.*[2] made *a*-Si:H/*a*-Si:H stacked tandem solar cells using several substrate temperatures (90–190 °C) and hydrogen dilutions (1–20). They reported an efficiency of 9.2% in the annealed state with a relative decrease of 8% in the efficiency after 900 h of light soaking. Von der Linden *et al.*[3] found in *a*-Si:H/*a*-Si:H modules an optimal thickness ratio of 1:6 between the top and bottom thicknesses depending on the total solar cell thickness. They determined the best thicknesses from light soaking experiments and measured less than a 10% relative decrease in the solar cell efficiency after 1000 h of light soaking. In these articles *a*-Si:H or combinations of *a*-Si:H and microcrystalline silicon (μc-Si) layers were used to build the tunnel recombination junction (TRJ).

Microcrystalline silicon (μc-Si) is a very interesting material to be used in tandem TRJ because its low mobility gap strongly favors recombination and its low optical absorption minimizes optical losses. These optoelectrical properties of μc-Si acted as a driving force to implement entire μc-Si tunnel junctions.[4–6] In this article, using computer modeling, we study in *a*-Si:H/*a*-Si:H tandem solar cells the kinetics controlling the electrical transport in their TRJ. We adopt as a baseline structure the following solar cell: SnO_2:F/*p*-*a*-SiC:H/*i*-*a*-Si:H/*n*-μc-Si:H/*p*-μc-Si:H/*i*-*a*-Si:H/*n*-*a*-Si:H/Ag. The record efficiency achieved at Utrecht University with this structure was 9.89%.[5] In order to reach these efficiencies interface oxidation treatments were needed at two interfaces: (a) *i*-*a*-Si:H/*n*-μc-Si:H and (b) *n*-μc-Si:H/*p*-μc-Si:H. The oxide layer at the *i*-*a*-Si:H/*n*-μc-Si:H interface improves the crystallinity of the *n*-μc-Si:H layer. In this article we show that the oxide layer at the *n*-μc-Si:H/*p*-μc-Si:H interface enhances recombination. We present experimental results for two different TRJ structures: *n*-μc-Si/oxide/*p*-μc-Si and *n*-μc-Si/*i*-μc-Si/*p*-μc-Si. In the last structure, the oxide layer was removed at the interface (b) but not at the interface (a). In our simulations we include trap assisted multistep tunneling recombination[7] and the Poole-Frenkel effect.[8]

II. TANDEM SOLAR CELL MODELING

A. General considerations

In this article we use the computer code D-AMPS, where D-AMPS stands for analysis of microelectronic and photonic devices (AMPS) core plus new developments. The computer code AMPS, described elsewhere,[9] was developed at The Pennsylvania State University. The new developments refer to new physics that were recently incorporated into AMPS by the first author of this manuscript. In tandem solar

cells we have to distinguish between ''good'' recombination taking place between electrons and holes photogenerated in the first and second cell, respectively, and ''bad'' recombination occurring between electrons and holes photogenerated in the same cell. Each electron–hole pair annihilated by good recombination contributes to the photocurrent. On the other hand, bad recombination occurring in *p*, *i*, and *n* layers reduces the total photocurrent leading to electrical losses. Back diffusion of electrons and holes at the front and back contact, respectively, are not significant loss mechanisms in tandem cells. If the tunnel or contact junction (TRJ) cannot provide enough good recombination, more carriers will recombine through bad recombination and the solar cell performance will deteriorate. Other undesired effects would be the creation of a light induced dipole due to the accumulation of trapped electrons and trapped holes what would weaken the electric field in the top cell, bottom cell, and in the TRJ intrinsic layers.

B. Previous work

In the last few years we can find several articles where *a*-Si:H based tandem or multijunction solar cells were modeled using computer codes where the Poisson's equation and the continuity equations were solved simultaneously with numerical techniques. The TRJ junctions of these *a*-Si:H based tandem cells were mostly made with *a*-Si:H. Research groups modeling these structures were forced to rely on complex and sophisticated approaches due to the high sensitivity of the tandem solar cell open circuit voltage (V_{oc}) to the mobility gap of the semiconductor used in the TRJ. Detailed studies demonstrate that standard electrical parameters of *a*-Si:H give rise to a good recombination of around 13–15 orders of magnitude lower than the one needed to reach the experimentally observed V_{oc}.[10] Reasonable values of V_{oc} cannot be achieved by only increasing the gap state density and capture cross sections. Hou *et al.*[11] and Bae and Fonash[12] showed enhancement of the good recombination in *a*-Si:H TRJ by adding a low mobility gap (LMG) and a highly defective layer between the *n*-*a*-Si:H and *p*-*a*-Si:H doped layers. On top of that they also graded the conduction band edge in the *n* layer and the valence band edge in the *p* layer toward the low mobility gap region. The LMG layer created the appropriate scenario to have a strong good recombination and the grading of both doped layers provided the diffusion gradient necessary to drive holes toward the LMG layer. Bruns *et al.*[1] used a slightly different approach, since they graded both mobility edges in each doped layer. They used mobility gaps as low as 0.52–1 eV in their LMG layers.

Willeman[13] incorporated trap assisted tunneling (TAT) recombination in tandem solar cell modeling. He implemented the model developed by Hurkx *et al.*,[7] which is an extension of the conventional Schockley–Read–Hall (SRH) model. Hurkx *et al.* defined electric field dependent factors that enhance the capture cross sections and the emission coefficients. Willeman found that the TAT approach increased the tandem solar cell V_{oc} but the predicted tandem $J-V$ curves were still considerably far from the measured characteristic. His studies indicated that the increase of the defect density of states and capture cross sections and the decrease of tunneling effective masses were not enough to successfully fit their experimental data. Although in the TAT approach the good recombination is significantly enhanced by a higher amount of free carriers available for recombination, electrons and holes still have to move to the physical position where the good recombination is taking place. A large gradient in the quasi-Fermi levels is still necessary to move these carriers or, in other words, a driving force for carrier transport must also be present. Hou *et al.*,[11] Bae and Fonash,[12] and Bruns *et al.*[1] implemented this driving force by grading the mobility gap. Willeman instead invoked to the exponential increase of the drift mobility μ_{eff} at electric field (E) intensities higher than 10^5 V/cm and showed that only when the TAT and the enhanced mobility models are simultaneously applied will the predicted tandem solar cell *J-V* curves by ASA (the computer code developed at Delft University, Netherlands) match the measured $J-V$ characteristics.

C. *a*-Si:H tandem solar cells having TRJ of μc-Si

The lower mobility gap of μc-Si naturally provides more good recombination than *a*-Si:H, making less stringent the requirements on the electrical parameters of the tandem TRJ. We used three different models in D-AMPS to model our TRJ: (a) the standard SRH recombination, (b) TAT recombination as proposed by Hurkx *et al.*,[7] and (c) the Poole–Frenkel (PF) effect[8] acting in conjunction with trap assisted tunneling (PFT) recombination. In the TAT approach, in regions where there is a high electric field, traps located at X_T can capture or emit free carriers from or to other locations different from X_T by tunneling. Tunneling transmission coefficients limiting transitions from extended to localized gap states are reduced by the presence of intense electric fields. This causes capture cross sections to become a function of the absolute value of the electric field by phonon-assisted tunneling.[7] The expressions of Hurkx *et al.*,[7] which depend only on local variables, can be expressed with analytical functions and add only two new electrical parameters: the electron and the hole effective mass.[7] The equations derived by Hurkx *et al.*[7] are strictly valid in regions where the electric field is constant. This assumption has to be fulfilled only in regions where tunneling currents are significant. The PF effect consists of a lowering in the potential barrier surrounding a localized state where a significant external electric field is present. The PF theory also predicts an enhancement in the emissions probabilities and in the capture cross sections of Coulomb centers due to the so-called field-induced barrier lowering.[8,14] The electric field in tandem TRJ could approach values near 10^6 V/cm that would give rise to a significant barrier lowering. The PF effect occurs only in processes where the trap is neutral when it is occupied by a carrier and charged when the carrier is emitted. For donor- or acceptor-like traps the PF effect is only active in processes of capture and emission of electrons in donor-like states and capture and emission of holes in acceptor-like states.[14] A similar statement can be made for amphoteric states.

In order to get started we will assume in this article that the TRJ μc-Si layers have uniform electrical properties and afterward we will briefly discuss the impact of the nonuniformity of μc-Si in the solar cell efficiency. The μc-Si mobility gap is assumed to be 1.2 eV. The μc-Si density of mid-gap states (DMS) is modeled using three amphoteric-like Gaussians (D^+, D^0, and D^-) which were centered at energies spaced by 0.3 eV and the correlation energy U has been assumed to be $U=0.2$ eV. The D^0 Gaussian is located at $U/2$ below midgap. The electron and hole mobilities adopted are 40 and 4 $\mathrm{cm^2\,V^{-1}\,s^{-1}}$.

In a TRJ having the simple n-μc-Si/p-μc-Si structure the ''good'' recombination between electrons and holes photogenerated in the first and second cells, respectively, takes place in a very narrow region (~30–40 Å) located near the n/p interface and mainly inside the p-μc-Si layer. In the rest of the μc-Si layers we have ''bad'' recombination. The region where good recombination takes place in a tandem solar cell can be established by inspecting the electron and hole current density profiles. Figure 1 shows the band diagram, the recombination rate, and the electron and hole current densities for this TRJ structure under short circuit conditions. In Fig. 1(b) we also plot the generation rate for comparison purposes. For this particular case the SRH formalism was adopted because the TAT model cannot be applied in regions where the electric field is highly nonuniform. Our results show that the position of the good recombination peak is not dictated by the asymmetry existing between the electron and hole mobility. This peak is instead sensitive to the asymmetry existing in the activation energies of the n-μc-Si and p-μc-Si layers. These activation energies were measured from temperature dependence of dark conductivity and found to be 26 and 50 meV for n-μc-Si and p-μc-Si, respectively. When the n-μc-Si and the p-μc-Si activation energies are exchanged in D-AMPS the position of the good recombination peak shifts from the p layer into the n layer. The good recombination peak is approximately located at the position where the Fermi level at thermodynamic equilibrium crosses midgap. The higher activation energy of the p-μc-Si layer causes the Fermi level to reach midgap inside of this region. The TRJ electric field and band diagram at thermodynamic equilibrium of a good designed tandem solar cell are not significantly modified by the presence of light or when a voltage bias is applied. The concentration of majority carriers at equilibrium present in both doped layers is already very high to be significantly perturbed by electrons and holes photogenerated in the cells and injected into the TRJ. We also observed very little dependence of V_{oc} with respect to n-μc-Si and p-μc-Si thicknesses (W_N and W_P) as long as W_N and W_P are equal to or higher than 20 nm. This result can be explained by looking at Figs. 1(b) and 1(c) where we see that most of the recombination taking place in μc-Si layers leads to electrical losses.

In order to enhance the good recombination, a thin oxide layer is usually grown at the n-μc-Si/p-μc-Si interface. This oxide layer is normally around 20–40 Å thick. Our working hypothesis is that this oxide layer increases the defect density near the oxide/μc-Si interfaces and can be easily tunneled through by both electrons and holes. In our previous articles[4,5] we modeled the presence of this oxide by adding a thin, undoped, and highly defective layer having the μc-Si mobility gap. This highly defective and low band-gap region enhanced the good recombination by shifting and pinning the Fermi level near midgap inside this region. The good recombination peak moves toward the n/p interface where the high DMS also favors good recombination. In principle, the same effect could be introduced by adding an intrinsic μc-Si layer inbetween the doped μc-Si layers. This intrinsic layer will force the Fermi level to cross midgap within this layer, but a low DMS could mitigate the good recombination rate and hurt the performance of the tandem solar cell. Figure 2 shows the band diagram, the recombination (and generation) rate, and the electron and hole current

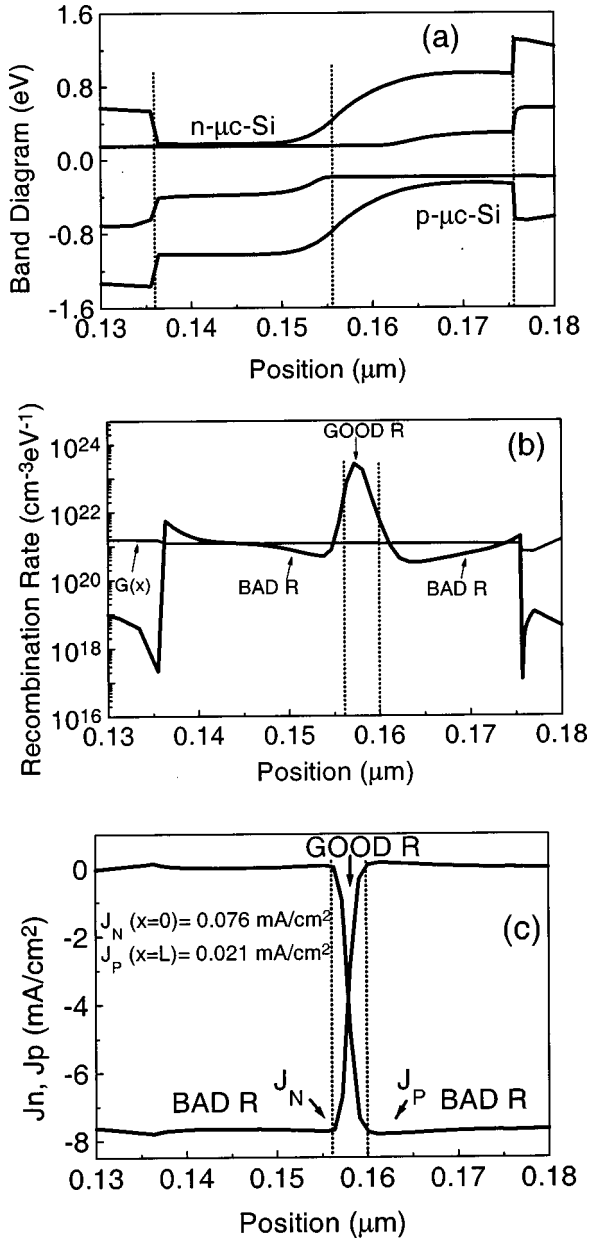

FIG. 1. (a) Band diagram, (b) recombination rate, and (c) electron and hole current densities of a μc-Si n-p tunnel recombination junction at short circuit conditions. $G(x)$ is the generation profile. Electron $[J_N(x=0)]$ and hole $[J_P(x=L)]$ back diffusion losses at the front and back contact, respectively, are also indicated.

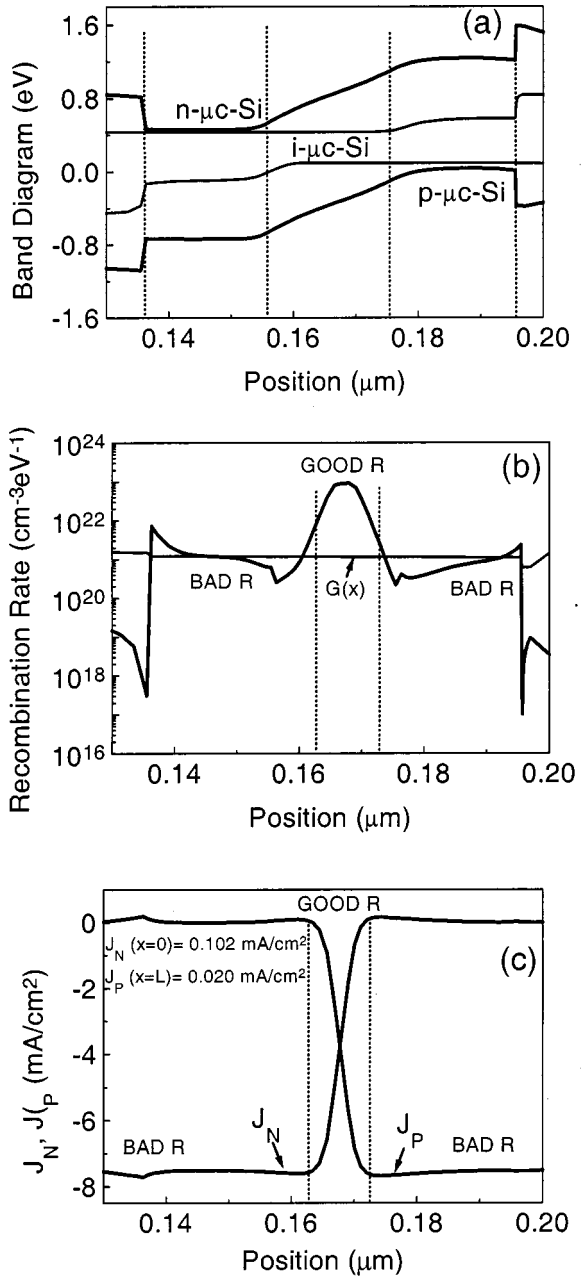

FIG. 2. (a) Band diagram, (b) recombination rate, and (c) electron and hole current densities of a μc-Si *n-i-p* tunnel recombination junction at short circuit conditions. The intrinsic layer is 20 nm thick. $G(x)$ is the generation profile. Electron $[J_N(x=0)]$ and hole $[J_P(x=L)]$ back diffusion losses at the front and back contact, respectively, are also indicated.

densities under short circuit condition of a μc-Si *n-i-p*TRJ having a 20 nm thick intrinsic layer. Figures 2(b) and 2(c) indicate that in n-μc-Si/i-μc-Si/p-μc-Si structures the good recombination spreads over most of the intrinsic layer instead of taking place only inside of a narrow region as in Figs. 1(b) and 1(c).

III. RESULTS AND DISCUSSION

In order to gain insight into the electrical transport taking place in the *n-i-p* μc-Si tunnel junction we have studied the dependence of the tandem cell efficiency with respect to the i-μc-Si layer thickness and its DMS. The DMS in

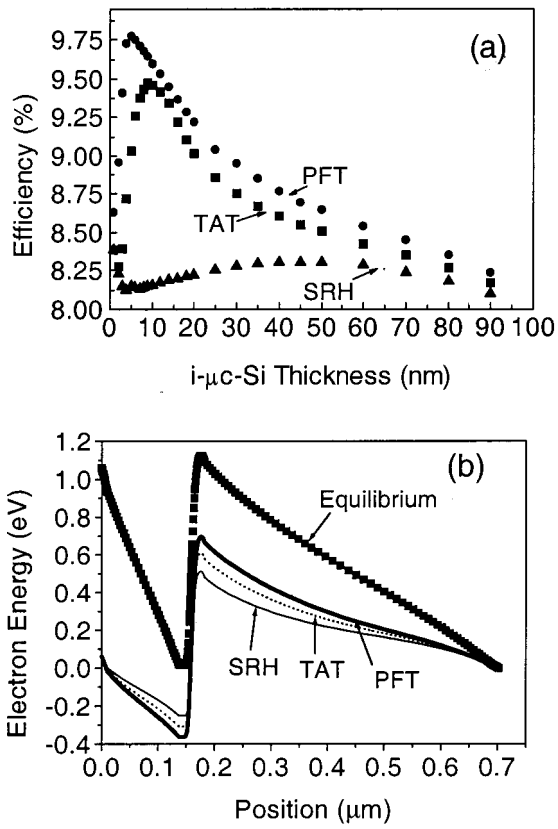

FIG. 3. (a) Dependence of the tandem solar cell efficiency with respect to the μc-Si *n-i-p* intrinsic layer thickness; (b) electron potential energy at equilibrium (squared symbols) and under AM1.5 light and 1.0 V forward bias voltage (solid lines) for a tandem solar cell having a 5 nm thick μc-Si intrinsic layer. The different models used are: the standard Schockley-Read-Hall recombination (SRH), trap assisted tunneling (TAT) recombination, and the Poole–Frenkel (PF) effect in conjunction with trap assisted tunneling recombination (PFT). The density of states in the i-μc-Si layer is $1.5 \times 10^{18}\,\mathrm{cm}^{-3}$.

both doped μc-Si layers has been adopted equal to $5.0 \times 10^{18}\,\mathrm{cm}^{-3}$. Figure 3(a) shows the tandem solar cell efficiency versus the i-μc-Si layer thickness. The DMS in the i-μc-Si layer has been adopted equal to $1.5 \times 10^{18}\,\mathrm{cm}^{-3}$ in order to fit some experimental results with the TAT approach that will be discussed below. We have to keep in mind that in μc-Si:H tunnel junctions the recombination rate is entirely controlled by midgap states because tails in μc-Si:H are very steep and μc-Si:H has a low mobility gap. At this point in our article we are only interested in capturing the main features predicted by the three models (SRH, TAT, and PFT) used in our simulations and just making general comparisons. Figure 3(a) shows that the standard SRH treatment gives rise to thickness dependent efficiencies. Very thin i-μc-Si layers cannot entirely hold good recombination that in *n-i-p* tunnel junctions spreads over a big portion of the intrinsic layer. Very thick i-μc-Si layers favor bad recombination. We see that the SRH model for μc-Si intrinsic layers thinner than 10 nm predicts that entirely removing the intrinsic layer is the best choice. The region where good recombination takes place moves inside the doped layers where there are more dangling bonds cooperating in the annihilation of electron–hole pairs. In order to show this effect

TABLE I. Power loss (mW/cm^2) occurring in the recombination junction for different i-μc-Si layer thicknesses (nm) at maximum power conditions. The lost power is shown for the three models used in this paper: Schockley–Read–Hall recombination (SRH), trap assisted tunneling (TAT) recombination, and Poole-Frenkel effect in conjunction with trap assisted tunneling (PFT) recombination.

Thickness (nm)	2	5	10	20	30
SRH (mW/cm^2)	2.025	2.114	2.144	1.985	1.858
TAT (mW/cm^2)	1.964	1.067	0.826	1.212	1.413
PFT(mW/cm^2)	1.220	0.294	0.366	0.527	0.746

the DMS in μc-Si doped layers was intentionally adopted slightly higher than in the intrinsic μc-Si layer. Figure 3(a) demonstrates that the TAT approach significantly enhances the predicted performance of the tandem cell. The inclusion of TAT shifts the highest solar cell efficiency to cells having much thinner i-μc-Si layers. Thinner i-μc-Si layers increase the electric field intensity, which enhances the tunneling probabilities. The maximum efficiency is obtained for i-μc-Si layer thickness within the range 6–10 nm depending upon the DMS adopted in this intrinsic layer. On the other hand, thicker i-μc-Si layers weaken the electric field, making tunneling less effective. For very thick i-μc-Si layers, the TAT and the SRH models predict the same efficiencies because we lose the electric field. Interestingly the inclusion of the PF effect in conjunction with trap assisted tunneling causes D-AMPS to predict the best solar cell efficiency at even thinner i-μc-Si layers. Figure 3(b) illustrates the energy potential profile of the tandem solar cell at equilibrium and under AM1.5 light and 1.0 V applied forward bias voltage of a tandem solar cell having a 5 nm μc-Si layer for the three different models used. Figure 3(b) clearly shows the presence of a superior transport in the recombination junction when either the TAT or the PFT model is invoked. Out of equilibrium we can see in Fig. 3(b) a considerably higher potential drop in the recombination junction that guarantees stronger electric fields in the collecting intrinsic layers. In Table I we list the power loss (mW/cm^2) occurring in the recombination junction for different i-μc-Si layer thicknesses (nm) at maximum power point conditions. This power loss indicates the potential gain in efficiency that can be further achieved in our tandem solar cell. We can see that the TAT and specially the PFT model minimize this undesired power loss in agreement with our results of Fig. 3.

Figure 4 illustrates the V_{oc} and fill factor (FF) dependence with respect to the i-μc-Si layer thickness. We can see the dramatic enhancement of V_{oc} when TAT is included in our modeling. The impact in the FF is much less impressive. The short circuit current J_{sc} not shown here is only slightly improved using the TAT and PFT models [for instances, for a i-μc-Si layer 5 nm thick the values of J_{sc} in mA/cm^2 are: 7.62 (SRH), 7.65 (TAT), and 7.67 (PFT)]. In the simulations shown in Fig. 3 we use the a-Si:H intrinsic layer thicknesses of the solar cells grown at our lab. In other words, in Fig. 3 a-Si:H intrinsic layer thicknesses were not adjusted to obtain the maximum of value of J_{sc}. A detailed model indicates that an enhancement in good recombination tends to reduce trapped and free carrier densities in the

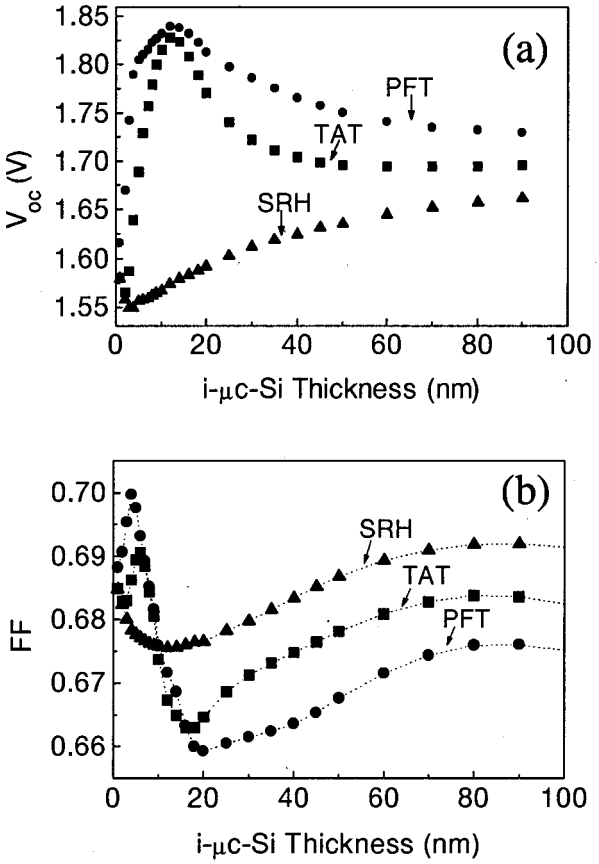

FIG. 4. Dependence of the tandem solar cell: (a) open circuit voltage and (b) fill factor with respect to the μc-Si n-i-p intrinsic layer thickness. The three models used are SRH, TAT, and PFT.

μc-Si doped layers in the regions near the n/i and i/p interfaces. As a result of that the electric fields inside the i-a-Si:H and i-μc-Si layers become strengthened, which favors even more good recombination inside the i-μc-Si layer and mitigates the effects of bad recombination in i-a-Si:H layers. This effect is minor at short circuit conditions but becomes quite significant at forward voltages leading to a dramatic improvement in the tandem solar cell V_{oc} [Fig. 4(a)].

The results of this section indicate that when PF and tunneling effects are included in our computer simulations, very thin i-μc-Si layers can be used in our TRJ to match the efficiencies experimentally observed. For low mobility gap materials, like μc-Si, computer modeling could guide us in selecting the most appropriate combination of DMS and thickness for the intrinsic layer. As we have already mentioned, the n-oxide-p is the most conventional TRJ configuration used in a-Si:H based tandem solar cells. We already mentioned that the inclusion of the oxide induces the formation of a highly defective layer (HDL) that enhances good recombination. However, using the n-oxide-p configuration, it is quite difficult to control the oxide thickness and the highly defective layer DMS and thickness. A very thick oxide could prevent free electrons and holes from tunneling through and very thick and defective HDL could also be detrimental. On the other hand, in the n-i-p configuration in

the TRJ we are able to have better control of the electrical parameters of the i-μc-Si layer, in particular on its DMS and thickness. This fact and the computer predictions shown in Figs. 3 and 4 encouraged us to fabricate a-Si:H based tandem solar cells where the n-oxide-p TRJ is replaced by a n-i-p μc-Si TRJ.

A. Experimental results

a-Si:H/a-Si:H tandem solar cells were made by plasma enhanced chemical vapor deposition in an ultrahigh vacuum multichamber system, PASTA. Cells were grown on Asahi U-type SnO_2 coated glass in the initial superstrate configuration SnO_2/p-a-SiC:H/i-a-Si:H/n-μc-Si:H/p-μc-Si:H/i-a-Si:H/n-a-Si:H/Ag. Our tandem solar cells were characterized with light $J-V$ and spectral response measurements at AM 1.5 illumination. The error in these measurements is within 3%.

An amorphous silicon tandem solar cell incorporating microcrystalline tunnel junction n-μc-Si:H/p-μc-Si:H yielded 10% efficiency in the annealed state.[4,5] The structural property of this microcrystalline junction was verified by the XTEM micrograph, which confirmed that these layers are highly crystalline.[5] The junction requires interface treatment (oxidation treatment) at two interfaces, namely before the n-μc layer and between the microcrystalline layers. Elastic recoil detection analysis confirmed the presence of oxygen peaks at these two interfaces[5] and showed that bonded oxygen at these sites is not etched away due to the hydrogen plasma of the overlying deposition. We assume that this bonded oxygen (suboxide) in the microcrystalline layer (at the junction interface) increases the density of defects. Oxygen induced defect creation has been reported in the literature.[15] Oxide treatment was done by CO_2 plasma at a low power (4 W) to avoid damage or even etching of the layer.

Having discussed the role of the oxide layer with computer modeling a-Si:H(1.88 eV)/a-Si:H(1.78 eV) tandem cells were also made by using thin intrinsic microcrystalline silicon as the interface layer in the tunnel junction in the configuration n-μc-Si(20 nm)/i-μc-Si(5 nm)/p-μc-Si (20 nm). The characteristics of this cell were compared with an a-Si:H(1.88 eV)/a-Si:H(1.78 eV) tandem cell using oxidation treatment at the junction n-μc-Si(20 nm)/oxide/p-μc-Si(20 nm). The oxide treatment before the n-μc layer was made in both tandem structures. Figure 5 shows the light $J-V$ curves of both tandem solar cells. It is clear from this figure that for the two cases the $J-V$ characteristics are very similar, with practically identical V_{oc}, J_{sc}, FF, and efficiency. The spectral responses (not shown here) are also very similar for both structures. These results give a direct confirmation to our previous modeling results and an indirect confirmation to the assumptions made in modeling the presence of an oxide layer. Thickness and deposition time of the intrinsic μc-Si layers can be carefully controlled to achieve consistent results. At present we do not have complete thickness variation of the intrinsic layer in TRJ. However preliminary studies on three thicknesses (2.5, 5, and 10 nm) revealed that the efficiency peaked at 5 nm and this is in conformity with the trend predictions of Fig. 3(a). As this is a sharp peak, careful thickness variation has to be made to obtain precise optimum thickness.

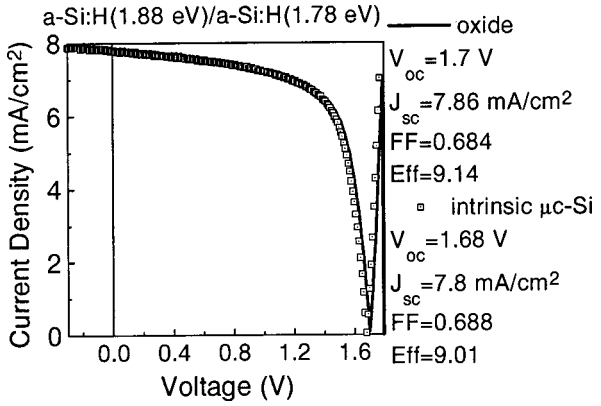

FIG. 5. Comparison of the experimental light $J-V$ curves of two tandem solar cells having the following μc-Si TRJ structures. n-oxide-p and n-i-p. The μc-Si intrinsic layer is 5 nm thick.

B. Fittings and parameter sensitivity studies

In order to use reliable parameters, we fitted the experimental light $J-V$ and the bias light QE response of tandem solar cells having the n-oxide-p or the n-i-p tunnel junction configuration. In Figs. 6 and 7 we show our fittings of the light $J-V$ and short circuit QE for a tandem solar cell having an n-i-p TRJ with a 5 nm thick intrinsic layer. These fittings were achieved with the PFT model and the resulting DMS in the i-μc-Si layer was $1.0\times10^{17}\,\mathrm{cm}^{-3}$. In order to reach the same fittings we need a DMS of $1.5\times10^{18}\,\mathrm{cm}^{-3}$ when the TAT model is used [see Fig. 3(a)] and a DMS of $1.3\times10^{19}\,\mathrm{cm}^{-3}$ when the SRH model is used. For a tandem solar cell having an n-oxide-p TRJ the same fittings are achieved for a DMS of $2.5\times10^{18}\,\mathrm{cm}^{-3}$ assuming that the HDL is 2 nm thick (this numbers stands for the PFT model). Taking a careful look at Fig. 6 we note that the slopes near J_{sc} and V_{oc} are slightly lower in our computer simulated light $J-V$ curve than in the experimental $J-V$ characteristic. These computer predicted slopes can be made steeper run-

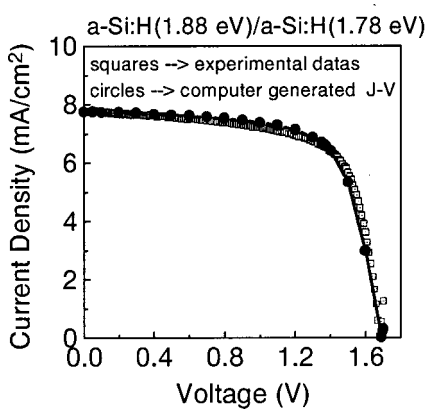

FIG. 6. Fitting of the tandem experimental light $J-V$ characteristic. The solar cell has a μc-Si n-i-p TRJ structure and the μc-Si intrinsic layer is 5 nm thick.

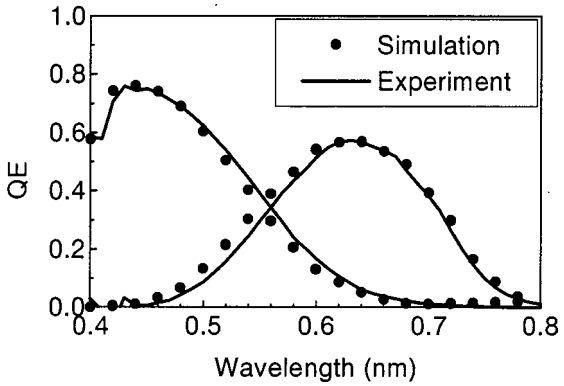

FIG. 7. Fitting of the tandem experimental spectral response (QE) characteristic. QE was measured at short circuit conditions. The solar cell has a μc-Si *n-i-p* TRJ structure and the μc-Si intrinsic layer is 5 nm thick.

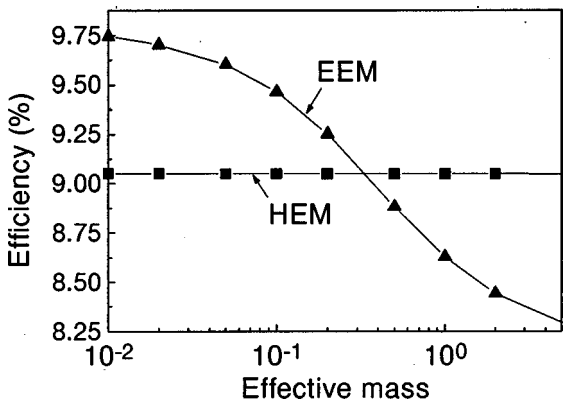

FIG. 9. Dependence of the tandem solar cell efficiency with respect to the μc-Si *n-i-p* intrinsic layer electron effective mass (EEM) and hole effective mass (HEM). In this figure the PFT model is used.

ning computer simulations with i-μc-Si mobility gaps below 1.2 eV but by doing that our predicted FF also becomes slightly off.

Using D-AMPS it is interesting to take a look at the dependence of the tandem solar cell efficiency with respect to the i-μc-Si DMS, free carrier mobilities, effective masses, and mobility gap. From now on we will use only the PFT model. Figure 8 illustrates the sensitivity of the solar cell efficiency to the i-μc-Si DMS. We can see that the efficiency does not necessarily keep improving upon an increase of the i-μc-Si DMS. In the extreme case of very high DMS ($>1.0\times10^{19}\,\mathrm{cm}^{-3}$) the defects could first distort and even cause the electric field to collapse inside the i-μc-Si layer bulk, which in turn would reduce the transmission tunneling probabilities and the effectiveness of the PF effect. We found that, as a rule of thumb, the product DMS and thickness at which the efficiency reaches its maximum is almost constant. For instance, the optimum efficiency is achieved for a DMS of $5.0\times10^{17}\,\mathrm{cm}^{-3}$ when the i-μc-Si layer is 20 nm thick, for a DMS of $1.0\times10^{18}\,\mathrm{cm}^{-3}$ when the i-μc-Si layer is 10 nm thick, and so on. For the parameters used in Figs. 6 and 7 the electric field inside the i-μc-Si layer is constant within 2.5%. The uniformity of the electric field can be better guaranteed for very thin i layers or for i layers having a much lower DMS than the doping densities used in the μc-Si:H doped layers.

Figure 9 shows the dependence of the solar cell efficiency upon the electron and the hole effective masses. In our previous simulations the electron and hole effective masses of i-μc-Si have been assumed to be equal to the effective masses of c-Si (0.33 and 0.55 respectively). As expected, the tandem solar cell efficiency is a strong function of the electron effective mass but curiously the same efficiency is a weak function of the hole effective mass within the range explored in Fig. 9. This result is originated by the lower activation energy present in n-μc-Si in comparison with the activation energy of p-μc-Si. Inside the i-μc-Si layer the good recombination peak is located closer to the i/p interface than to the n/i interface, which causes the barrier to be tunneled by electrons to be thicker than the barrier to be tunneled by holes. This means that recombination in midgap states is limited by the electron supply. When we exchange the activation energies of these μc-Si doped layers we note that with D-AMPS the solar cell efficiency is a strong function of the hole effective mass and a weak function of the electron effective mass.

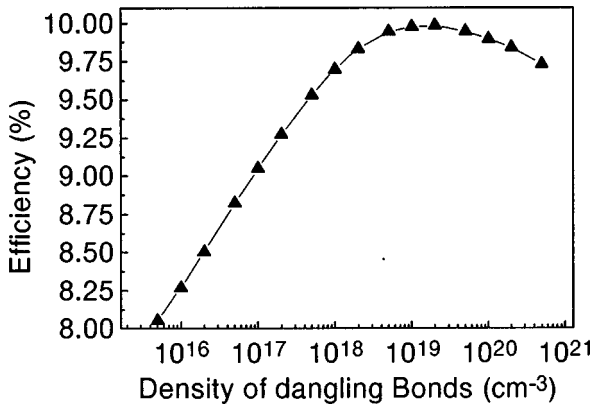

FIG. 8. Dependence of the tandem solar cell efficiency with respect to the μc-Si *n-i-p* intrinsic layer density of midgap states (DMS). In this figure the PFT model is used.

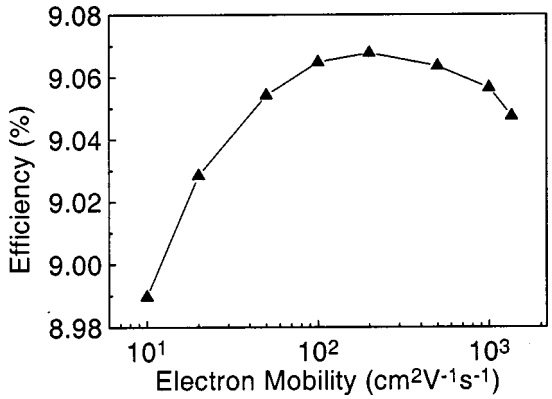

FIG. 10. Dependence of the tandem solar cell efficiency with respect to the μc-Si *n-i-p* intrinsic layer electron (*UN*) and hole (*UP*) mobility. Here the PFT model is used.

TABLE II. Tandem solar cell V_{oc}, FF and efficiencies for different μc-Si mobility gaps assuming a DMS of $1.0\times10^{17}\,cm^{-3}$. Last row corresponds to the density of mid-gap states (DMS) needed to achieve an efficiency of 9.02% for the different μc-Si mobility gaps.

Gap (eV)	1.20	1.25	1.30	1.35	1.40	1.45	1.50
V_{oc} (V)	1.690	1.652	1.632	1.603	1.574	1.538	1.496
FF	0.689	0.686	0.681	0.674	0.666	0.657	0.648
Efficiency	9.021	8.775	8.604	8.367	8.117	7.824	7.505
DMS (cm^{-3})	1.0×10^{17}	2.5×10^{17}	5.0×10^{17}	1.75×10^{18}	5.0×10^{18}[a]	—	—

[a]The achieved efficiency for this gap was 8.99%.

The tandem solar cell efficiency shows a minor dependence upon the free carrier mobilities of i-μc-Si. In Fig. 10 we illustrate this dependence keeping an electron–hole mobility ratio of 10 except for the highest mobility shown in this figure, which corresponds to typical c-Si free carrier mobilities. Higher mobilities on both doped μc-Si layers in conjunction with higher mobilities in i-μc-Si do not result in better solar cell performances.

The mobility gap of μc-Si is lower than the mobility gap of a-Si:H and its value is not very well known. This novel material raises an interesting question in tandem solar cell modeling: ''which is the highest mobility gap that we can use in μc-Si TRJ and still fit our experimental results?'' In order to answer this question we used the PFT approach, which is our most developed model. In Table II we list the i-μc-Si DMS needed to fit the light $J-V$ of our tandem solar cell having the n-i-p TRJ configuration where the intrinsic layer is 5 nm thick. The μc-Si mobility gap in doped and intrinsic layers is adopted equally.

This table shows that the experimental light $J-V$ cannot be successfully matched with D-AMPS when the μc-Si mobility gap is higher than 1.4 eV. The constant increase of DMS does not lead us to higher efficiencies. We already have problems reaching an efficiency of 9.02% when the μc-Si mobility gap is only 1.4 eV. A DMS of 5.0×10^{18} gives rise to an efficiency of 8.99% and higher values of DMS give rise to lower solar cell efficiencies due to a drop in FF. Within the range explored in Table II, J_{sc} does not show significant changes upon the increase of μc-Si mobility gap.

C. Final comments

Raman spectroscopy indicates that thin layers of μc-Si grown on a-Si:H have nonuniform electrical and optical properties.[16] The first few nanometers show amorphous character and only above several nanometers is the fully crystalline phase achieved. In our materials we have observed this transition in around 40–50 nm. Assuming an exponential decrease of the mobility gap with distance our preliminary results indicate that the most important features of the kinetics and transport physics of μc-Si TRJ can still be captured by assuming that the μc-Si layers have uniform electrical properties. Using nonuniform electrical properties we also observe that the peak of good recombination is located in the doped layer having the higher activation energy. Recombination (bad and good) goes mainly through the regions where the μc-Si mobility is minimum and V_{oc} becomes a stronger function of the doped layer thicknesses than when the μc-Si mobility is assumed constant. TAT and PFT models also predict that the highest tandem solar cell efficiencies are achieved for intrinsic μc-Si layers of a few nanometers. This issue will be discussed in detail in a future publication.

IV. CONCLUSIONS

Tandem solar cells in the superstrate configuration SnO_2:F/p-a-SiC:H/i-a-Si:H/tunnel junction/i-a-Si:H/n-a-Si:H/Ag were modeled and made by using two different tunnel junction structures: n-μc-Si:H/oxide/p-μc-Si:H and n-μc-Si:H/i-μc-Si:H/p-μc-Si:H. Both modeling predictions and experimental findings confirmed that physical properties of the oxidized microcrystalline interface are similar to the ones of a highly defective intrinsic silicon layer and that comparable efficiencies can be reached by using either one or the other tunnel junction. This study also shows an alternative and more reproducible method to make a tunnel recombination junction, namely by using an intrinsic silicon interface layer. The experimental tandem solar cell efficiency depends strongly on the intrinsic μc-Si:H layer thickness in agreement with the predictions of our modeling when trap assisted multistep tunneling recombination is included to describe transport inside the tunnel junction. Even by taking into account Poole–Frenkel the experimental tandem illuminated $J-V$ characteristics cannot be successfully fitted for μc-Si:H mobility gap values higher than 1.4 eV.

ACKNOWLEDGMENTS

The authors highly appreciate the financial support of Netherlands Organization for Energy and Environment (NOVEM), and of Agencia Nacional de Promoción Científica y Tecnológica, Proyect No. 10-00000-0095. They also thank Karine van der Werf for depositions.

[1] J. Bruns, M. Choudhury, and H. G. Wageman, Proceedings of 13th European Photovoltaic Solar Energy Conference, Nice, 1995, p. 230.
[2] S. Wieder, B. Rech, C. Beneking, F. Siebke, W. Reetz, and H. Wagner. Proceedings of 13th European Photovoltaic Solar Energy Conference, 1995, p. 234.
[3] M. B. von der Linden, J. Hyvärinen, W. Loyer, and R. E. I. Schropp, 13th European Photovoltaic Solar Energy Conference, 1995, p. 284.
[4] J. K. Rath, F. A. Rubinelli, and R. E. I. Schropp, J. Non-Cryst. Solids **227–230**, 1202 (1998).
[5] J. K. Rath, F. A. Rubinelli, and R. E. I. Schropp, Proceedings of 2nd World Conference and Exhibition on Photovoltaic Solar Energy Conversion, Viena, 1998, p. 812.
[6] J. Yang, A. Banerjee, and S. Guha, *Amorphous and Microcrystalline Silicon Technology*, edited by S. Wagner, M. Hack, E. A. Schiff, R. Schropp and I. Shimizu (1997), Vol. 467, p. 693.

[7] G. A. M. Hurkx, D. B. M. Klassen, and M. P. G. Knuvers, IEEE Trans. Electron Devices **29**, 331 (1992).
[8] G. Vincent, A. Chantre, and D. Bois, J. Appl. Phys. **50**, 5484 (1979).
[9] P. Chatterjie, P. J. McElheny, and S. J. Fonash, J. Appl. Phys. **67**, 3803 (1990).
[10] J. Y. Hou, thesis in Engineering Science and Mechanics, The Pennsylvania State University, 1993.
[11] J. Y. Hou, J. K. Arch, S. J. Fonash, S. Wiedeman, and M. Bennett, Proceedings 22th IEEE PVSC, 1991, p. 1260.
[12] S. Bae and S. J. Fonash, Proceedings of 1st WCPEC PVSC, Hawaii, 1994, p. 484.
[13] J. A. Willemen, Ph.D thesis, Technische Universiteit Delft, 1998.
[14] O. K. B. Lui and P. Migliorato, Solid-State Electron. **41**, 575 (1997).
[15] D. Will, C. Lerner, W. Fuhs, and K. Lips, *Amorphous and Microcrystalline Silicon Technology*, edited by S. Wagner, M. Hack, E. A. Schiff, R. Schropp and I. Shimizu (1997), Vol. 467, p. 361.
[16] J. K. Rath, J. Wallinga, and R. E. I. Schropp, *Amorphous Silicon Technology*, edited by M. Hack, E. A. Schiff, S. Wagner, R. Schropp and A. Matsuda (1996), Vol. 420, p. 271.